Comparative Genomics of *Campylobacter iguaniorum* to Unravel Genetic Regions Associated with Reptilian Hosts

Maarten J. Gilbert[1], William G. Miller[2], Emma Yee[2], Marja Kik[3], Aldert L. Zomer[1,4], Jaap A. Wagenaar[1,4,5], and Birgitta Duim[1,4,*]

[1]Department of Infectious Diseases and Immunology, Faculty of Veterinary Medicine, Utrecht University, Utrecht, The Netherlands

[2]Produce Safety and Microbiology Research Unit, Agricultural Research Service, U.S. Department of Agriculture, Albany, California, USA

[3]Department of Pathobiology, Faculty of Veterinary Medicine, Utrecht University, Utrecht, The Netherlands

[4]WHO Collaborating Center for Campylobacter/OIE Reference Laboratory for Campylobacteriosis, Utrecht, The Netherlands

[5]Central Veterinary Institute of Wageningen UR, Lelystad, The Netherlands

*Corresponding author: E-mail: b.duim@uu.nl.

Accepted: August 31, 2016

Abstract

Campylobacter iguaniorum is most closely related to the species *C. fetus*, *C. hyointestinalis*, and *C. lanienae*. Reptiles, chelonians and lizards in particular, appear to be a primary reservoir of this *Campylobacter* species. Here we report the genome comparison of *C. iguaniorum* strain 1485E, isolated from a bearded dragon (*Pogona vitticeps*), and strain 2463D, isolated from a green iguana (*Iguana iguana*), with the genomes of closely related taxa, in particular with reptile-associated *C. fetus* subsp. *testudinum*. In contrast to *C. fetus*, *C. iguaniorum* is lacking an S-layer encoding region. Furthermore, a defined lipooligosaccharide biosynthesis locus, encoding multiple glycosyltransferases and bounded by *waa* genes, is absent from *C. iguaniorum*. Instead, multiple predicted glycosylation regions were identified in *C. iguaniorum*. One of these regions is > 50 kb with deviant G + C content, suggesting acquisition via lateral transfer. These similar, but non-homologous glycosylation regions were located at the same position on the genome in both strains. Multiple genes encoding respiratory enzymes not identified to date within the *C. fetus* clade were present. *C. iguaniorum* shared highest homology with *C. hyointestinalis* and *C. fetus*. As in reptile-associated *C. fetus* subsp. *testudinum*, a putative tricarballylate catabolism locus was identified. However, despite colonizing a shared host, no recent recombination between both taxa was detected. This genomic study provides a better understanding of host adaptation, virulence, phylogeny, and evolution of *C. iguaniorum* and related *Campylobacter* taxa.

Key words: *Campylobacter iguaniorum*, reptile, comparative genomics, recombination, phylogeny, evolution.

Introduction

The majority of the *Campylobacter* species are associated with endothermic mammalian and avian hosts. Recently, a novel *Campylobacter* species has been described, *Campylobacter iguaniorum* (*Cig*), which is predominantly isolated from ectothermic reptilian hosts (Gilbert et al. 2015). Chelonians and lizards in particular appear to be a primary reservoir of this *Campylobacter* species. Reported overall prevalence in reptiles based on culturing was 8.2%; 15.6% of the chelonians and 6.1% of the lizards, but none of the snakes examined, carried this *Campylobacter* species (Gilbert et al. 2014a). Recently, *Cig* has also been isolated from a non-reptilian host (Miller et al. 2016a).

Within the genus *Campylobacter*, this species forms a clearly separated phylogenetic clade, together with the closely related taxa *C. fetus*, *C. hyointestinalis*, and *C. lanienae* (collectively called the *C. fetus* clade). *C. fetus* currently comprises three subspecies: mammal-associated *C. fetus* subsp. *fetus* (*Cff*) and *C. fetus* subsp. *venerealis* (*Cfv*), and reptile-associated *C. fetus* subsp. *testudinum* (*Cft*) (Fitzgerald et al. 2014). As with *Cig*, *Cft* has been shown to be associated primarily with reptiles, and both taxa are the most frequently isolated *Campylobacter* in reptiles (Harvey and Greenwood 1985; Wang et al. 2013; Gilbert et al. 2014a). Also, *C. hyointestinalis* has been infrequently isolated from reptiles (Gilbert et al. 2014a). Interestingly, *Campylobacter* species commonly

found in various avian and mammalian hosts, such as *C. coli*, *C. jejuni*, and *C. lari*, were not isolated from reptiles, despite culturing conditions suitable for these species. It was speculated that the host body temperature, which is on average lower and more fluctuating in reptiles than in mammals and birds, is associated with this remarkable species distribution (Gilbert et al. 2014a). Indeed, *Cig*, *C. fetus*, and to a lesser extent *C. hyointestinalis*, were found able to grow at lower temperatures than most other *Campylobacter* species (Gilbert et al. 2015).

The pathogenicity of *Cig* in reptiles is unknown; isolates have been recovered both from reptiles with and without clinical signs of disease (Benejat et al. 2014; Gilbert et al. 2014a). In contrast to reptile-associated *Cft*, which has been shown to cause infection in humans (Tu et al. 2004; Patrick et al. 2013), no human *Cig* infections have been reported to date.

The first closed and annotated *Cig* genome has been described previously (Gilbert et al. 2014b). Genome analysis and comparison provide valuable insights into host adaptation, virulence, phylogeny, and evolution of this reptile-associated *Campylobacter* species. Comparison with reptile-associated *Cft* could identify factors specific for adaptation to their shared reptilian host. Here we report the complete whole genome sequences of two *Cig* strains isolated from reptiles, and compare them to those of the closely related taxa *Campylobacter fetus*, *C. hyointestinalis*, and *C. lanienae*.

Campylobacter iguaniorum genome features and comparison

The genome size of strain 1485E is 1,684,608 bp with a 70,030 bp megaplasmid; strain 2364D is 1,809,624 bp with an estimated 54,764 bp megaplasmid. The general features of *Cig* strains 1485E and 2463D are summarized in supplementary table S1, Supplementary Material online.

Multiple genomic regions were specific for *Cig*, i.e. no orthologs were identified in all or most members of the *C. fetus* clade or the entire *Campylobacter* genus. In total, 59 genes were conserved in both *Cig* strains, which were absent from all other *C. fetus* clade members (supplementary table S2, Supplementary Material online). Multiple genes involved in sulfur metabolism were identified, indicating that this is important in *Cig* biology. Indeed, phenotypic testing showed that *Cig* and *C. hyointestinalis* are one of the few *Campylobacter* species that produce H_2S on sulfate containing TSI agar (Gilbert et al. 2015). Notably, the gene coding for L-lactate permease (*lctP*) was absent from *Cig* and *C. hyointestinalis* subsp. *hyointestinalis*, but was well conserved in the other *C. fetus* clade members and most other *Campylobacter* species. In *C. jejuni*, transport of L-lactate occurs primarily via LctP, although at least one other transport route also exists (Thomas et al. 2011). This predicts that *Cig* relies less on exogenous L-lactate as carbon or energy source than other *Campylobacter* species encoding *lctP*.

Several genes were found to be shared specifically by both reptile-associated taxa *Cig* and *Cft* (supplementary table S2, Supplementary Material online). As in reptile-associated *Cft*, a putative tricarballylate catabolism locus *tcuRABC* (CIG1485E_0479-0482; CIG2463D_0480-0483) was identified in both *Cig* strains. This locus is partially present in *C. hyointestinalis* subsp. *lawsonii*, but as *tcuC* is a truncated pseudogene, it is likely not functional. Tricarballylate could potentially be used as a carbon and energy source by *Cig*, as this locus has been shown to function in the catabolism of tricarballylate (a citrate analog) (Lewis et al. 2004). Tricarballylate is considered to cause grass tetany in ruminants, a disease characterized by acute magnesium deficiency. In the ruminant rumen, *trans*-aconitate present in grass is rapidly reduced to tricarballylate, a toxic end product of ruminal fermentation (Russell 1985). Neither the ruminant nor the normal rumen flora can catabolize tricarballylate efficiently. However, it has been shown that *Salmonella enterica* serovar Typhimurium strain LT2 can use tricarballylate as a carbon and energy source; the end product of tricarballylate metabolism is *cis*-aconitate, which then enters into the citric acid cycle (Gutnick et al. 1969; Lewis et al. 2004). Conservation of the *tcuRABC* locus in the reptile-associated taxa suggests that tricarballylate is ubiquitous in the niche inhabited by *Cig* and *Cft*, i.e., the mucosa of the reptilian intestines. As the *tcuRABC* locus is present in all highly prevalent reptile-associated *Campylobacter* taxa, this locus could confer an advantage in colonization of the reptilian host.

In contrast to most *Campylobacter* species, both *Cig* strains lack a defined lipooligosaccharide (LOS) region, bounded by *waa* genes and containing multiple glycosyltransferases (supplementary table S2, Supplementary Material online). The lack of *waaDEF*, which are highly conserved in *Campylobacter* and *Arcobacter*, is especially remarkable. Instead, multiple separate predicted glycosylation regions were identified (fig. 1). A large glycosylation region (>50 kb) was present in both strains. Although syntopic in both strains, large parts of this region were not homologous and, in combination with the deviant G+C content (29.0–30.0%), suggests acquisition via lateral transfer. However, this region was highly homologous in strain 2463D and *C. hyointestinalis* subsp. *hyointestinalis*. In strains 1485E and 2463D, respectively 20.6% (7/34) and 22.0% (9/41) of the GC tracts were identified within this glycosylation region.

As in other *Campylobacter* species many of the hypervariable GC tracts reside in surface structure-related genes showing phase variation. However, in strains 1485E and 2463D, respectively 23.5% (8/34) and 20.0% (8/41) of the GC tracts were located within autotransporter domain-containing genes, whose role in *Cig* biology remains to be determined. In total, seven autotransporter domain-containing genes were found conserved in both strains and showed no or low

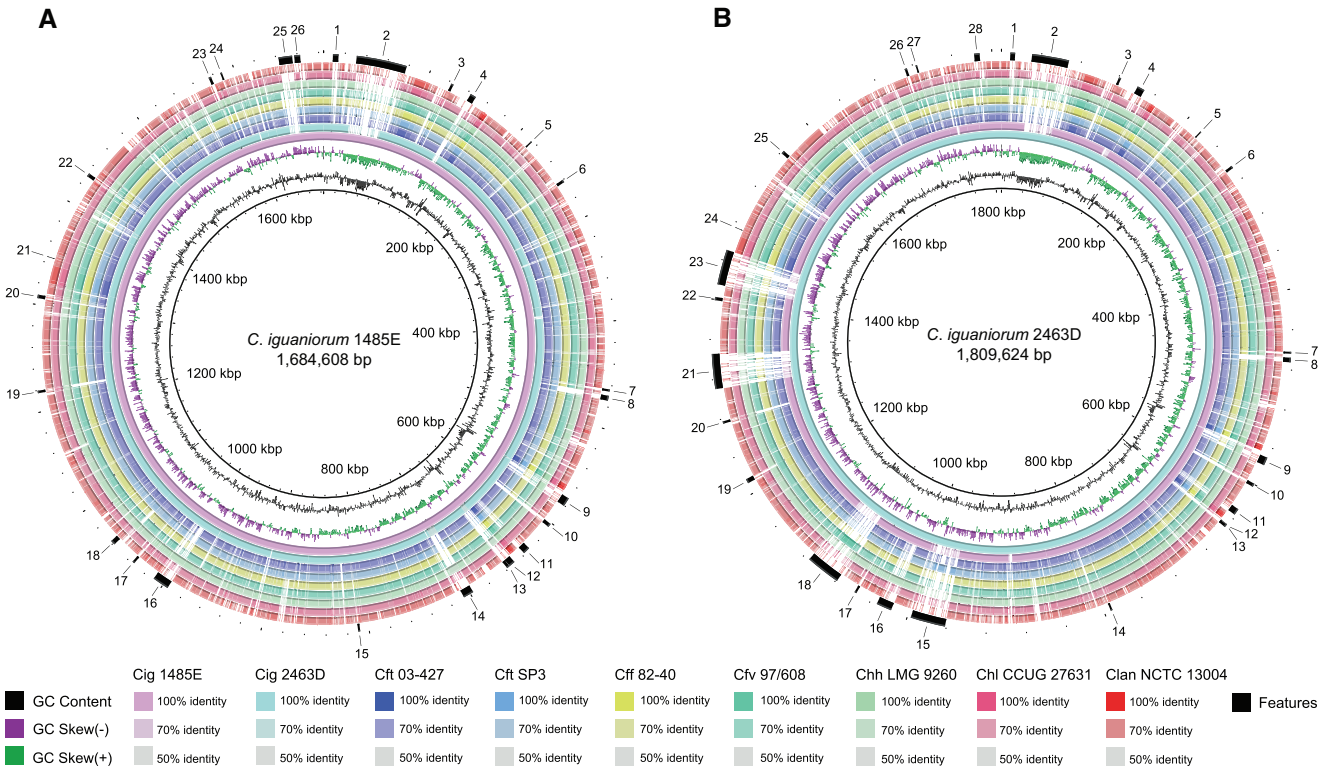

Genomic features		Locus tag CIG1485E
1	autotransporter domain protein	CIG1485E_0008-0009
2	glycosylation region	CIG1485E_0024-0066
3	putative lipoprotein region	CIG1485E_0128-0130
4	glycosylation region	CIG1485E_0147-0153
5	xanthine/uracil/vitamin C permease	CIG1485E_0224
6	L-serine catabolism operon	CIG1485E_0275-0276
7	autotransporter domain protein	CIG1485E_0473
8	tricarballylate catabolism region *tcuRABC*	CIG1485E_0479-0482
9	CRISPR-associated protein region	CIG1485E_0588-0595
10	autotransporter domain protein	CIG1485E_0617
11	polysulfide reductase region	CIG1485E_0639-0644
12	CRISPR repeat region	n/a
13	autotransporter domain protein	CIG1485E_0654
14	CRISPR repeat region	n/a
15	autotransporter domain protein	CIG1485E_0796
16	cytochrome c nitrite reductase containing region	CIG1485E_0986-1000
17	autotransporter domain protein	CIG1485E_1021
18	ABC-type spermidine/putrescine transport system	CIG1485E_1149-1153
19	autotransporter domain protein	CIG1485E_1223
20	putative arsenic resistance region	CIG1485E_1309-1313
21	shikimate kinase AroL	CIG1485E_1352
22	putative iron ABC transporter region	CIG1485E_1439-1441
23	autotransporter domain protein	CIG1485E_1594
24	sulfatase family protein	CIG1485E_1607
25	glycosylation region	CIG1485E_1671-1687
26	sulfate permease containing region	CIG1485E_1691-1695

Genomic features		Locus tag CIG2463D
1	autotransporter domain protein	CIG2463D_0008-0009
2	glycosylation region	CIG2463D_0024-0063
3	putative lipoprotein region	CIG2463D_0131-0133
4	flavocytochrome c region	CIG2463D_0150-0156
5	xanthine/uracil/vitamin C permease	CIG2463D_0229
6	L-serine catabolism operon	CIG2463D_0280-0281
7	autotransporter domain protein	CIG2463D_0474
8	tricarballylate catabolism region *tcuRABC*	CIG2463D_0480-0483
9	CRISPR-associated protein region	CIG2463D_0588-0595
10	autotransporter domain protein	CIG2463D_0617
11	polysulfide reductase region	CIG2463D_0639-0644
12	CRISPR repeat region	n/a
13	autotransporter domain protein	CIG2463D_0654
14	autotransporter domain protein	CIG2463D_0797
15	putative prophage	CIG2463D_0964-1017
16	cytochrome c nitrite reductase containing region	CIG2463D_1039-1053
17	autotransporter domain protein	CIG2463D_1074
18	genomic island (Vir region)	CIG2463D_1101-1138
19	ABC-type spermidine/putrescine transport system	CIG2463D_1240-1244
20	autotransporter domain protein	CIG2463D_1314
21	putative prophage	CIG2463D_1349-1390
22	putative arsenic resistance region	CIG2463D_1442-1446
23	putative prophage	CIG2463D_1457-1513
24	shikimate kinase AroL	CIG2463D_1543
25	putative iron ABC transporter region	CIG2463D_1632
26	autotransporter domain protein	CIG2463D_1791
27	sulfatase family protein	CIG2463D_1804
28	sulfate permease containing region	CIG2463D_1872-1876

Fig. 1.—BRIG plots of *C. iguaniorum* and most closely related *Campylobacter* species. BLASTN-based genomic comparison of *C. iguaniorum* strains 1485E and 2463D, *C. fetus* subsp. *testudinum* (Cft) strains 03-427 and SP3, *C. fetus* subsp. *fetus* (Cff) strain 82-40, *C. fetus* subsp. *venerealis* (Cfv) strain 97/608, *C. hyointestinalis* subsp. *hyointestinalis* (Chh) strain LMG 9260, *C. hyointestinalis* subsp. *lawsonii* (Chl) strain CCUG 27631, and *C. lanienae* (Clan) strain NCTC 13004. Characteristic features of *C. iguaniorum* have been highlighted. Reference genome is *C. iguaniorum* strain 1485E (*A*); reference genome is *C. iguaniorum* strain 2463D (*B*).

homology with other *Campylobacter* species. Noteworthy, 89% (8/9) of the autotransporter domain-containing genes in both strains contained a GC tract.

The *cas* genes present in *Cig* were homologous with those in *C. hyointestinalis* subsp. *hyointestinalis*, but not with those in *C. fetus*, indicating that at least two different CRISPR/Cas systems are present within the *Campylobacter fetus* clade (fig. 1).

One of the characteristics shared by *Cig*, *C. fetus*, and most *Arcobacter* species is the ability to grow at lower temperatures (≤25 °C) than most other *Campylobacter* species (On et al. 1996; Gilbert et al. 2015). Also, these species have been shown to occur together in reptilian hosts, which often show a broad body temperature range and on average lower body temperatures compared with most endothermic mammals and birds (Gilbert et al. 2014a). As in *C. fetus*, but in contrast to *C. jejuni* in which *nuoE* and *nuoF* are lacking (Kelly 2008), all NADH:quinone oxidoreductase complex I subunits (NuoA-N) are present in *Cig*, suggesting that NADH is an important electron donor in this species. Interestingly, NuoA-N present in *Cig* and all other *C. fetus* clade members showed higher homology to species from the *Arcobacter* genus (≤72%), than to other species from the *Campylobacter* genus (≤55%). The high homology observed in the NADH:quinone oxidoreductase complex I subunits might be related to low temperature adaptation. Indeed, in other organisms NADH:quinone oxidoreductase complex I is considered the most thermolabile protein complex of oxidative phosphorylation (Downs and Heckathorn 1998). Within the *Campylobacter* genus, the ability to exclusively proliferate at lower temperatures (18–37 °C) is unique for *Cig*. This feature may have helped *Cig* colonize hosts which have a low and variable body temperature.

Campylobacter iguaniorum phylogeny and diversity

A phylogenomic reconstruction accounting for the effects of homologous recombination was performed, based on a 1,042,737 nucleotide gapless alignment of the whole genomes of *Cig* and most closely related species *C. fetus*, *C. hyointestinalis*, and *C. lanienae* (supplementary fig. S1, Supplementary Material online). *Cig* was clearly distinct from the other *Campylobacter* species. The first split occurred between *C. lanienae* and the other species. Excluding the more distantly related *C. lanienae*, the branch lengths indicated that *Cig* is less related to the last common ancestor than the other species. Interestingly, *Cig*, *C. fetus*, and *C. hyointestinalis* branch of the last common ancestor at the same point, suggesting that these species started diverging at the same time.

In order to examine the genomic relatedness in further detail, the average nucleotide identity (ANI) was determined for the whole genomes of both *Cig* strains and strains of the most closely related taxa *C. fetus*, *C. hyointestinalis*, and *C. lanienae* (supplementary table S3, Supplementary Material online). ANI values were highest for *Cig* and both *C. hyointestinalis* and *C. fetus*. Homology was higher between *Cig* and reptile-associated *Cft* than between *Cig* and mammal-associated *C. fetus* subspecies *fetus* and *venerealis*, indicating that both reptile-associated taxa *Cig* and *Cft* share genomic regions, which might be associated with adaptation to their shared reptilian hosts. Higher ANI values between *Cig* strain 2463D and *Cft* strain SP3, *C. fetus* subsp. *venerealis*, and *C. hyointestinalis* subsp. *hyointestinalis* can be explained by shared laterally transferred genomic regions, such as prophages, and shared glycosylation regions (fig. 1). In addition to this, the genes shared by *Cig* and other members of the *C. fetus* clade (≥50% identity) showed that most genes were shared between *Cig* and *C. hyointestinalis* subsp. *hyointestinalis*, followed by both *Cft* strains, suggesting that these taxa are most closely related (supplementary table S4, Supplementary Material online). Nevertheless, on a species level, differences based on shared genes and ANI are small and in support of the whole genome-based phylogeny showing similar divergence between *Cig*, *C. fetus*, and *C. hyointestinalis*.

MLST analysis of 18 *Cig* strains showed two distinct lineages and a high intraspecies diversity without any identical sequence type (fig. 2). No clear association with host type was observed, as *Cig* isolates originating from lizards and chelonians were found in both lineages. Nevertheless, host association was observed at the species level to some degree, as *Cig* isolates originating from animals of the same species, but from different locations were mostly clustering together. This was most clear in *Iguana iguana*, in which two *Cig* isolates, which were obtained from different animals in 2003 and 2012, clustered closely together. In contrast, two isolates obtained from the same animal (11S02571-1 and 11S02571-4) showed a large genetic distance, indicating that *Cig* diversity within the same animal can be high.

Both *Cig* and *Cft* colonize the same reptilian hosts (Gilbert et al. 2014a), facilitating potential lateral gene transfer between these two taxa. Indeed, both reptile-associated taxa share specific genomic regions which might confer certain competitive advantages to survive in the reptilian host. Furthermore, similar prophages were identified in the accessory genomes of both taxa, which can serve as a vehicle for novel genetic material and enable gene flow between both taxa. However, no recent recombination events between both taxa were detected in the core genomes. Despite the close genetic relationship and shared host type, the recombination rate between both reptile-associated taxa can be considered low compared with certain other *Campylobacter* species colonizing a shared host (Sheppard et al. 2008). This could be explained by a recent introduction in the same host or by barriers such as an intrinsic resistance to interspecific recombination or separated niches within the host, as has been shown for *C. jejuni* (Sheppard et al. 2014). Instead, multiple regions showed higher than expected homology in

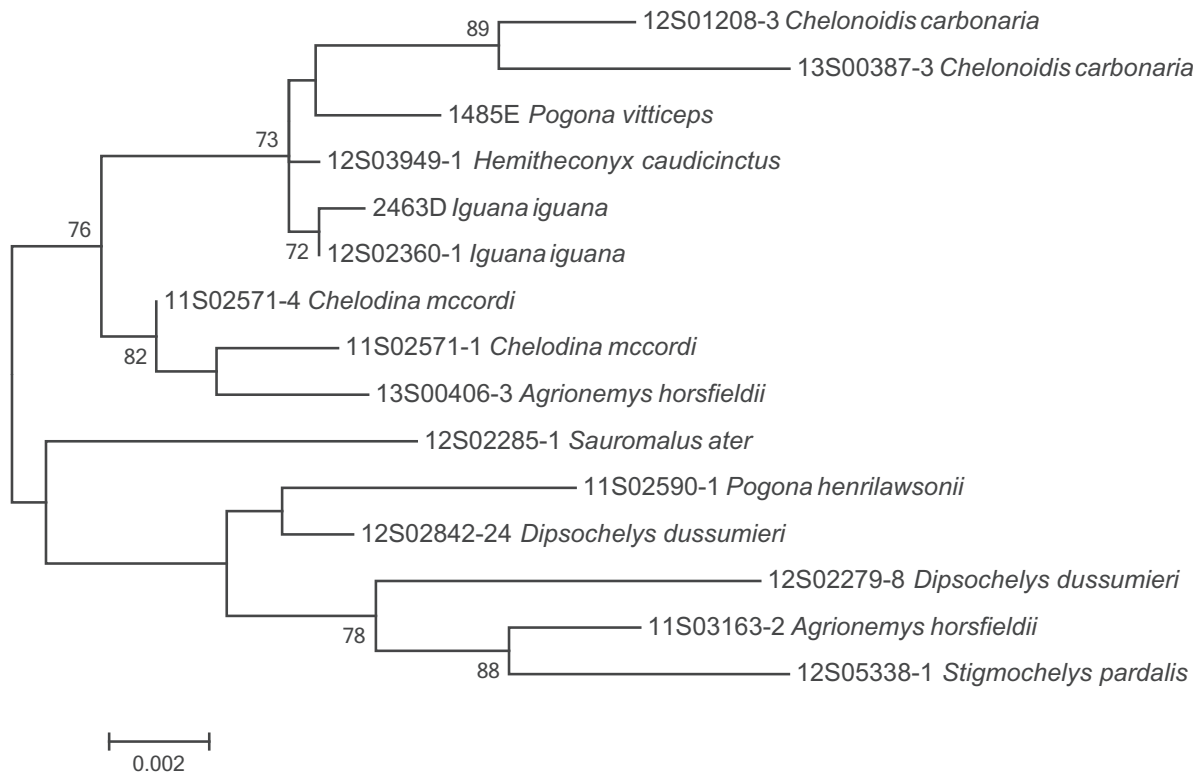

Fig. 2.—Maximum likelihood dendrogram of *C. iguaniorum* based on concatenated MLST sequences, using 500 bootstraps. Isolate numbers are followed by the host species.

C. iguaniorum, *C. hyointestinalis*, and members of the *C. concisus* clade, suggesting gene flow between these distantly related *Campylobacter* taxa.

Material and Methods

Strains

Characteristics of all strains used in this study are summarized in table 1. *Cig* strain 1485E (= CCUG 66346 = LMG 28143) was isolated in 2003 from a bearded dragon (*Pogona vitticeps*) with a hypertrophic and perforated colon. *Cig* strain 2463D (= CCUG 66347) was isolated in 2003 from a green iguana (*Iguana iguana*) with chronic interstitial nephritis. All strains were grown on Columbia agar with 5% sheep blood (Oxoid, the Netherlands) in a microaerobic atmosphere (83.3 N_2, 7.1% CO_2, 3.6% H_2, and 6% O_2) at 37 °C for 48 h.

Whole Genome Sequencing

The sequencing of *Cig* strains 1485E and 2463D was performed using shotgun and paired-end reads obtained on a Roche 454 FLX Genome Sequencer. A total of 292,658 (1485E) or 318,374 (2463D) 454 reads were assembled using the Newbler assembler (v2.6) into single chromosomal scaffolds of 12 (1485E) or 11 (2463D) unique contigs and single megaplasmid scaffolds, providing draft genome sequences with coverages of 68× (1485E) or 65× (2463D). All 454 base calls were validated using 1,570,644 (1485E) or 2,300,370 (2463D) Illumina MiSeq reads, providing an additional 178× (1485E) or 263× (2463D) coverage. Scaffold gaps were filled as described (Merga et al. 2013). Sequences across the contig junctions were confirmed with Sanger sequencing. Assembly was confirmed using PacBio long reads for strain *Cig* 2463D. PacBio RS reads were assembled into contigs using Quiver (Pacific Bioscience, Menlo Park, CA, USA). Homopolymeric GC tracts were characterized using the high-depth MiSeq reads.

Genome Analysis

Protein-, rRNA-, and tRNA-encoding genes were identified as described (Merga et al. 2013). The 1485E genome was annotated based on *Cft* strain 03-427^T (accession number CP006833) (Gilbert et al. 2013; Fitzgerald et al. 2014) and the annotation of the 2463D genome was based on that of 1485E, with further annotation using Artemis (Rutherford et al. 2000), the identification of Pfam domains (v.27.0) (Finn et al. 2014), and BLASTP comparisons to proteins in the NCBI non-redundant (nr) database. CRISPR regions were identified using CRISPRFinder (Grissa et al. 2007). The

Table 1
Features of the *Campylobacter* Strains Used in this Study

Species	Strain	Source organism	Source type	Location	Sequence data	Sequence method	Reference	Accession number
Cig	1485E	Lizard (*Pogona vitticeps*)	Feces	NL	WGS	454, Illumina, PacBio	Gilbert et al. 2014b	CP009043-CP009044
Cig	2463D	Lizard (*Iguana iguana*)	Feces	NL	WGS	454, Illumina, PacBio	Gilbert et al. 2015	CP010995
Cig	11S02571-1	Chelonian (*Chelodina mccordi*)	Feces	NL	MLST	Sanger	Gilbert et al. 2014a	KU697811, KU697824, KU697837, KU697850, KU697863, KU697876, KU697889
Cig	11S02571-4	Chelonian (*Chelodina mccordi*)	Feces	NL	MLST	Sanger	Gilbert et al. 2014a	KU697812, KU697825, KU697838, KU697851, KU697864, KU697877, KU697890
Cig	11S02590-1	Lizard (*Pogona henrilawsonii*)	Feces	NL	MLST	Sanger	Gilbert et al. 2014a	KU697813, KU697826, KU697839, KU697852, KU697865, KU697878, KU697891
Cig	11S03163-2	Chelonian (*Agrionemys horsfieldii*)	Feces	NL	MLST	Sanger	Gilbert et al. 2014a	KU697814, KU697827, KU697840, KU697853, KU697866, KU697879, KU697892
Cig	12S01208-3	Chelonian (*Chelonoidis carbonaria*)	Feces	NL	MLST	Sanger	Gilbert et al. 2014a	KU697815, KU697828, KU697841, KU697854, KU697867, KU697880, KU697893
Cig	12S02279-8	Chelonian (*Aldabrachelys gigantea*)	Feces	NL	MLST	Sanger	Gilbert et al. 2014a	KU697816, KU697829, KU697842, KU697855, KU697868, KU697881, KU697894
Cig	12S02285-1	Lizard (*Sauromalus ater*)	Feces	NL	MLST	Sanger	Gilbert et al. 2014a	KU697817, KU697830, KU697843, KU697856, KU697869, KU697882, KU697895
Cig	12S02360-1	Lizard (*Iguana iguana*)	Feces	NL	MLST	Sanger	Gilbert et al. 2014a	KU697818, KU697831, KU697844, KU697857, KU697870, KU697883, KU697896
Cig	12S02842-24	Chelonian (*Aldabrachelys gigantea*)	Feces	NL	MLST	Sanger	Gilbert et al. 2014a	KU697819, KU697832, KU697845, KU697858, KU697871, KU697884, KU697897
Cig	12S03949-1	Lizard (*Hemitheconyx caudicinctus*)	Feces	NL	MLST	Sanger	Gilbert et al. 2014a	KU697820, KU697833, KU697846, KU697859, KU697872, KU697885, KU697898
Cig	12S05338-1	Chelonian (Stigmochelys pardalis)	Feces	FR	MLST	Sanger	Benejat et al. 2014	KU697821, KU697834, KU697847, KU697860, KU697873, KU697886, KU697899
Cig	13S00387-3	Chelonian (*Chelonoidis carbonaria*)	Feces	NL	MLST	Sanger	Gilbert et al. 2014a	KU697822, KU697835, KU697848, KU697861, KU697874, KU697887, KU697900
Cig	13S00406-3	Chelonian (*Agrionemys horsfieldii*)	Feces	NL	MLST	Sanger	Gilbert et al. 2014a	KU697823, KU697836, KU697849, KU697862, KU697875, KU697888, KU697901
Cff	82-40	Human	Blood	US	WGS	Sanger	Perez et al. 1985	CP000487
Cft	03-427	Human	Blood	US	WGS	454, Illumina, PacBio	Gilbert et al. 2013	CP006833
Cft	SP3	Snake (*Heterodon nasicus*)	Feces	UK	WGS	454, Illumina, PacBio	Gilbert et al. 2016	CP010953
Cfv	97/608	Bovine	Placenta	AR	WGS	454, Illumina, PacBio	van der Graaf-van Bloois et al. 2014	CP008810-CP008812
Chh	LMG 9260	Human	Feces	BE	WGS	454, Illumina	Miller et al. 2016b	CP015575
Chl	CCUG 27631	Porcine	Gastric biopsy	SE	WGS	454, Illumina	Miller et al. 2016b	CP015576
Clan	NCTC 13004	Human	Feces	SE	WGS	454	Logan et al. 2000	CP015578

Cig, C. iguaniorum; Cff, C. fetus subsp. fetus; Cft, C. fetus subsp. testudinum; Cfv, C. fetus subsp. venerealis; Chh, C. hyointestinalis subsp. hyointestinalis; Chl, C. hyointestinalis subsp. lawsonii; Clan, C. lanienae. AR, Argentina; BE, Belgium; FR, France; NL, Netherlands; SE, Sweden; UK, United Kingdom; US, United States. MLST, multilocus sequence typing; WGS, whole genome sequencing.

complete annotated genome sequence of *Cig* strain 1485E has been deposited in GenBank under accession numbers CP009043 (chromosome) and CP009044 (megaplasmid) (Gilbert et al. 2014b). The complete annotated genome sequence of the *Cig* strain 2463D chromosome has been deposited in GenBank under accession number CP010995. Accession numbers of all genomes used in this study can be found in table 1.

The *C. iguaniorum* strain 1485E genome was compared with the genome of strain 2463D and the completed genomes of the closely related taxa *C. fetus* subsp. *testudinum* (strains 03-427 and SP3), *C. fetus* subsp. *fetus* (strain 82-40), *C. fetus* subsp. *venerealis* (strain 97/608), *C. hyointestinalis* subsp. *hyointestinalis* (strain LMG 9260), *C. hyointestinalis* subsp. *lawsonii* (strain CCUG 27631), and *C. lanienae* (NCTC 13004). For *Campylobacter* species outside the *C. fetus* clade, BLASTP comparisons to proteins in the NCBI non-redundant (nr) database were performed. A local BLAST was performed based on the predicted proteomes of all genomes and the results were screened for features specific for one or both *Cig* strains and the other members of the *C. fetus* clade. Using JSpecies v.1.2.1 (Richter and Rosselló-Móra 2009) and BLAST v.2.2.26, average nucleotide identity (ANI) values based on the whole genome sequences were calculated for these strains as a measure of genetic relatedness. The BLAST parameters were: X = 150, q = −1, F = F, e = 1e−15, and a = 2. To visualize genomic regions specific for *Cig*, the BLAST ring image generator (BRIG) (Alikhan et al. 2011) was used, based on BLAST v.2.2.26.

Orthologous Grouping and Phylogenomic Reconstruction

An all versus all BLAST was performed for all predicted proteins of the whole genomes (table 1) at an E-value cutoff of 1E−6. To determine the orthologous relationships of all proteins, the BLAST output was parsed by Orthagogue (Ekseth et al. 2014). Proteins were considered for orthology clustering if the proteins had at least 50% identity and at least 50% overlap. To determine the orthologous groups, Markov clustering (MCL) was performed using MCL-edge (Enright et al. 2002). Genes encoding the proteins were aligned with each other within their respective orthologous groups using MUSCLE (Edgar 2004). A super alignment was created by concatenating the aligned genes according to their position in *Cig* strain 1485E if they were present in all isolates. Gaps were removed using Gblocks (Castresana 2000). Based on this super alignment phylogenomic reconstruction and prediction of recombination events was performed using Gubbins (Croucher et al. 2014) with the default settings. Phylogenetic dendrograms were created using Fasttree (Price et al. 2009). A BLAST search of the predicted recombination regions of both *Cig* strains against the genes of *Cft* was performed to search for particular recombination between these reptile-associated taxa.

MLST

Multilocus sequence typing (MLST) was performed for all *Cig* strains listed in table 1. The MLST loci were extracted from the genomes of 1485E and 2463D and sequenced as described previously for the other *Cig* isolates (Miller et al. 2012). For HFglt, the annealing temperature was lowered to 46 °C and 40 instead of 35 cycles were used. Sequences were trimmed and concatenated. In MEGA v.6.06, the concatenated sequences were aligned using MUSCLE and a Maximum likelihood dendrogram was created using 500 bootstraps. Accession numbers of the MLST sequence data can be found in table 1.

Supplementary Material

Supplementary tables S1–S4 and figure S1 are available at *Genome Biology and Evolution* online (http://www.gbe.oxfordjournals.org/).

Acknowledgments

We thank Linda van der Graaf-van Bloois for valuable advice and Arjen Timmerman for technical support. We thank Mary Chapman and Nathaniel Simon for the generation of Illumina MiSeq reads and assistance in the final assembly and genome closure. This work was partially supported by USDA-ARS CRIS project 5325-42000-047-00D.

Literature Cited

Alikhan N, Petty NK, Zakour NLB, Beatson SA. 2011. BLAST Ring Image Generator (BRIG): simple prokaryote genome comparisons. BMC Genomics 12:402.

Benejat L, et al. 2014. Characterization of a *Campylobacter fetus*-like strain isolated from the faeces of a sick leopard tortoise (*Stigmochelys pardalis*) using matrix-assisted laser desorption/ionization time of flight as an alternative to bacterial 16S rDNA phylogeny. Lett. Appl. Microbiol. 58:338–343.

Castresana J. 2000. Selection of conserved blocks from multiple alignments for their use in phylogenetic analysis. Mol. Biol. Evol. 17:540–552.

Croucher NJ, et al. 2014. Rapid phylogenetic analysis of large samples of recombinant bacterial whole genome sequences using Gubbins. Nucleic Acids Res. 43:e15.

Downs CA, Heckathorn SA. 1998. The mitochondrial small heat-shock protein protects NADH: ubiquinone oxidoreductase of the electron transport chain during heat stress in plants. FEBS Lett. 430:246–250.

Edgar RC. 2004. MUSCLE: multiple sequence alignment with high accuracy and high throughput. Nucleic Acids Res. 32:1792–1797.

Ekseth OK, Kuiper M, Mironov V. 2014. orthAgogue: an agile tool for the rapid prediction of orthology relations. Bioinformatics 30:734–736.

Enright AJ, Van Dongen S, Ouzounis CA. 2002. An efficient algorithm for large-scale detection of protein families. Nucleic Acids Res. 30:1575–1584.

Finn RD, et al. 2014. Pfam: the protein families database. Nucleic Acids Res. 42:D222–D230.

Fitzgerald C, et al. 2014. Description of *Campylobacter fetus* subsp. *testudinum* subsp. nov., isolated from humans and reptiles. Int. J. Syst. Evol. Microbiol. 64:2944–2948.

Gilbert MJ, et al. 2013. Complete genome sequence of *Campylobacter fetus* subsp. *testudinum* strain 03-427^T. Genome Announc. 1:e01002–e01013.
Gilbert MJ, et al. 2014a. Occurrence, diversity, and host association of intestinal *Campylobacter*, *Arcobacter*, and *Helicobacter* in reptiles. PLoS One 9:e101599.
Gilbert MJ, et al. 2014b. Complete genome sequence of *Campylobacter iguaniorum* strain 1485E^T, isolated from a bearded dragon (*Pogona vitticeps*). Genome Announc. 2:e00844–14.
Gilbert MJ, Kik M, Miller WG, Duim B, Wagenaar JA. 2015. *Campylobacter iguaniorum* sp. nov., isolated from reptiles. Int. J. Syst. Evol. Microbiol. 65:975–982.
Gilbert MJ, et al. 2016. Comparative genomics of *Campylobacter fetus* from reptiles and mammals reveals divergent evolution in host-associated lineages. Genome Biol. Evol. 8:2006–2019.
Grissa I, Vergnaud G, Pourcel C. 2007. CRISPRFinder: a web tool to identify clustered regularly interspaced short palindromic repeats. Nucleic Acids Res. 35:W52–W57.
van der Graaf-van Bloois L, et al. 2014. Inconsistency of phenotypic and genomic characteristics of *Campylobacter fetus* subspecies requires re-evaluation of current diagnostics. J. Clin. Microbiol. 52:4183–4188.
Gutnick D, Calvo JM, Klopotowski T, Ames BN. 1969. Compounds which serve as the sole source of carbon or nitrogen for *Salmonella typhimurium* LT-2. J. Bacteriol. 100:215–219.
Harvey S, Greenwood JR. 1985. Isolation of *Campylobacter fetus* from a pet turtle. J. Clin. Microbiol. 21:260–261.
Kelly DJ. 2008. Complexity and versatility in the physiology and metabolism of *Campylobacter jejuni*. In: Nachamkin I, Szymanski CM, Blaser MJ, editors. Campylobacter. Washington D.C.: ASM Press. p. 41–61.
Lewis JA, Horswill AR, Schwem BE, Escalante-Semerena JC. 2004. The tricarballylate utilization (*tcuRABC*) genes of *Salmonella enterica* serovar Typhimurium LT2. J. Bacteriol. 186:1629–1637.
Logan JM, Burnens A, Linton D, Lawson AJ, Stanley J. 2000. *Campylobacter lanienae* sp. nov., a new species isolated from workers in an abattoir. Int. J. Syst. Evol. Microbiol. 50:865–872.
Merga JY, Winstanley C, Williams NJ, Yee E, Miller WG. 2013. Complete genome sequence of the *Arcobacter butzleri* cattle isolate 7h1h. Genome Announc. 1:e00655–13.
Miller WG, et al. 2012. Multilocus sequence typing methods for the emerging *Campylobacter* species *C. hyointestinalis*, *C. lanienae*, *C. sputorum*, *C. concisus*, and *C. curvus*. Front. Cell Infect. Microbiol. 2:45.
Miller WG, Yee E, Huynh S, Chapman MH, Parker CT. 2016a. Complete genome sequence of the *Campylobacter iguaniorum* strain RM11343, isolated from an alpaca. Genome Announc. 4:e00646–e00616.
Miller WG, Yee E, Chapman MH. 2016b. Complete genome sequences of *Campylobacter hyointestinalis* subsp. *hyointestinalis* strain LMG 9260 and *Campylobacter hyointestinalis* subsp. *lawsonii* strain LMG 15993. Genome Announc. 4:e00665–16.
On SL, Holmes B, Sackin MJ. 1996. A probability matrix for the identification of campylobacters, helicobacters and allied taxa. J. Appl. Bacteriol. 81:425–432.
Patrick ME, et al. 2013. Human infections with new subspecies of *Campylobacter fetus*. Emerg. Infect. Dis. 19:1678–1680.
Perez GI, Hopkins JA, Blaser MJ. 1985. Antigenic heterogeneity of lipopolysaccharides from *Campylobacter jejuni* and *Campylobacter fetus*. Infect. Immun. 48:528–533.
Price MN, Dehal PS, Arkin AP. 2009. FastTree: computing large minimum evolution trees with profiles instead of a distance matrix. Mol. Biol. Evol. 26:1641–1650.
Richter M, Rosselló-Móra R. 2009. Shifting the genomic gold standard for the prokaryotic species definition. Proc. Natl. Acad. Sci. U S A. 106:19126–19131.
Russell JB. 1985. Enrichment and isolation of rumen bacteria that reduce trans-aconitic acid to tricarballylic acid. Appl. Environ. Microbiol. 49:120–126.
Rutherford K, et al. 2000. Artemis: sequence visualization and annotation. Bioinformatics 16:944–945.
Sheppard SK, et al. 2014. Cryptic ecology among host generalist *Campylobacter jejuni* in domestic animals. Mol. Ecol. 23:2442–2451.
Sheppard SK, McCarthy ND, Falush D, Maiden MC. 2008. Convergence of *Campylobacter* species: implications for bacterial evolution. Science 320:237–239.
Thomas MT, et al. 2011. Two respiratory enzyme systems in *Campylobacter jejuni* NCTC 11168 contribute to growth on L-lactate. Environ. Microbiol. 13:48–61.
Tu ZC, et al. 2004. *Campylobacter fetus* of reptile origin as a human pathogen. J. Clin. Microbiol. 42:4405–4407.
Wang CM, Shia WY, Jhou YJ, Shyu CL. 2013. Occurrence and molecular characterization of reptilian *Campylobacter fetus* strains isolated in Taiwan. Vet. Microbiol. 164:67–76.

Associate editor: Howard Ochman